The Canadian Mineralogist
Vol. 50, pp. 471-479 (2012)
DOI: 10.3749/canmin.50.2.471

STOICHIOMETRIC ARSENOPYRITE, FeAsS, FROM LA ROCHE-BALUE QUARRY, LOIRE-ATLANTIQUE, FRANCE: CRYSTAL STRUCTURE AND MÖSSBAUER STUDY

LUCA BINDI

Museo di Storia Naturale, Sezione di Mineralogia – Università di Firenze, via La Pira 4, I–50121 Firenze, Italy, and C.N.R., Istituto di Geoscienze e Georisorse, Sezione di Firenze, Via La Pira 4, I–50121 Firenze, Italy

YVES MOËLO[§], PHILIPPE LÉONE AND MICHEL SUCHAUD

Institut des Matériaux Jean Rouxel (IMN), Université de Nantes, CNRS, 2, rue de la Houssinière, BP 32229, F–44322 Nantes Cedex 3, France

ABSTRACT

Arsenopyrite from La Roche-Balue quarry (Loire-Atlantique department, France), with the stoichiometric composition FeAsS, has been studied by X-ray single-crystal diffraction and ^{57}Fe Mössbauer spectroscopy. Its unit cell is *a* 5.7612(8), *b* 5.6841(7), *c* 5.7674(8) Å, β 111.721(8)°, and *V* 175.46(4) Å^3 (Z = 4). Taking into account very fine ubiquitous twinning on {101}, its crystal structure has been refined in the space group $P2_1/c$ on the basis of 758 unique reflections [$F_o > 4\sigma(F_o)$] to R_1 = 0.0298. Within uncertainty limits, it indicates three unmixed Fe, As and S positions. The ^{57}Fe Mössbauer spectrum of this arsenopyrite shows two broad absorption peaks that were fitted using the superposition of three doublets denoted as A, B and C, with parameters relative to area *S*, isomer shift δ, and quadrupole splitting ΔE_Q, as follows: S_A 82.2%, δ_A 0.24(1) mm/s, ΔE_{QA} 1.12(2) mm/s; S_B 8.5%, δ_B 0.25(1) mm/s, ΔE_{QB} 0.69(2) mm/s; S_C 9.3%, δ_C 0.26(1) mm/s, ΔE_{QC} 1.49(2) mm/s. This set of values agrees well with the most recently published results for arsenopyrite samples with a composition close to stoichiometry. The three distinct Fe positions indicated by Mössbauer spectroscopy are not visible in the X-ray study. Whereas the main doublet A would seem to correspond to the $FeAs_3S_3$ octahedron of the ideal structure, the two minor doublets B and C, with a ΔE_Q shift towards marcasite and löllingite, respectively, may be due to local disorder (*e.g.*, twin contact walls) changing the octahedral coordination of Fe to unequal As:S ratios.

Keywords: arsenopyrite, crystal structure, Mössbauer study, iron coordination, La Roche-Balue, France.

SOMMAIRE

L'arsénopyrite de la carrière de La Roche-Balue, dans le département de la Loire-Atlantique, France, qui présente une composition stœchiométrique FeAsS, a été étudiée par diffraction X sur monocristal ainsi que par spectroscopie Mössbauer de ^{57}Fe. Sa maille élémentaire (groupe spatial $P2_1/c$) est *a* 5.7612(8), *b* 5.6841(7), *c* 5.7674(8) Å, β 111.721(8)°, *V* 175.46(4) Å^3 (Z = 4). En prenant en compte un très fin maclage ubiquiste selon {101}, sa structure a été résolue sur la base de 758 réflexions uniques [$F_o > 4\sigma(F_o)$] avec R_1 = 0.0298. Elle indique dans la limite des incertitudes de mesure trois sites purs à Fe, As et S. Le spectre Mössbauer de ^{57}Fe montre deux pics d'absorption élargis, qui ont été ajustés sur la base de la somme de trois doublets A, B et C, avec comme valeurs de leurs paramètres (surface relative *S*, déplacement isomérique *d*, et éclatement quadripolaire ΔE_Q): S_A 82.2%, d_A 0.24(1) mm/s, ΔE_{QA} 1.12(2) mm/s; S_B 8.5%, d_B 0.25(1) mm/s, ΔE_{QB} 0.69(2) mm/s; S_C 9.3%, d_C 0.26(1) mm/s, ΔE_{QC} 1.49(2) mm/s. Cette combinaison est en plein accord avec les données publiées récemment sur des échantillons d'arsénopyrite proches de la stœchiométrie. Les trois différentes positions du fer révélées par étude Mössbauer ne sont pas visibles aux rayons X. Tandis que le doublet principal A correspondrait à l'octaèdre $FeAs_3S_3$ de la structure idéale, les deux doublets secondaires B et C, montrant un décalage de ΔE_Q vers la marcasite et la pyrite, respectivement, seraient tributaires d'un désordre à échelle locale (par exemple les parois de contact des domaines de macle), qui modifierait la coordinence du fer vers des rapports As:S dissymétriques.

Mots-clés: arsénopyrite, structure cristalline, étude Mössbauer, coordinence du fer, La Roche-Balue, France.

§ *E-mail address*: Yves.Moelo@cnrs-imn.fr

Introduction

Arsenopyrite is common in various types of sulfide deposits, together with pyrite and pyrrhotite, and may constitute a major ore mineral in some deposits, particularly orogenic gold ores. In such ores, it is the main carrier of gold, which appears as micro-inclusions or as "invisible" gold, either as metal nano-inclusions, or in solid solution in the arsenopyrite structure. Despite its importance in gold deposits, and potential concerns in environmental geochemistry due to the negative impact of arsenopyrite as the main source of arsenic in soil pollution, crystal-chemical studies of arsenopyrite are relatively rare. The relative paucity of structural data contrasts with the vast amount of chemical data showing the variability of arsenopyrite composition. Its general formula can be written as $(Fe,Co,Ni)(As,Sb)_{1+x}(S,Se)_{1-x}$; according to numerous electron-microprobe data, which are confirmed by the experimental study of Kretschmar & Scott (1976), there is a strong nonstoichiometry in the As:S ratio, with x varying from less from 0.05 down to –0.14 (Cipriani *et al.* 1998).

After the first structural study by Buerger (1936), a detailed crystal-chemical study of arsenopyrite was performed by Morimoto & Clark (1961), who took into account chemical composition and nonstoichiometry, crystal data (unit cell and structure) and twinning. The crystal structure was solved using a sulfur-rich sample from Freiberg, Germany. More recently, Fuess *et al.* (1987) examined another sample of S-rich arsenopyrite from Hakansboda, Sweden, in which a high Co content is present (structural formula: $Fe_{0.87}Co_{0.13}As_{0.88}S_{1.12}$). Murzin *et al.* (2003) carried out ^{57}Fe Mössbauer spectroscopic studies on various samples of arsenopyrite from two gold deposits. These spectra revealed unexpected complexities, mainly related to the coexistence of several non-equivalent positions of Fe.

In the context of numerous electron-microprobe analyses performed on arsenopyrite from various French sulfide vein deposits, we selected a sample from La Roche-Balue quarry (Loire-Atlantique department, France) as a chemical standard, in view of its purity, homogeneity, and composition close to the stoichiometric formula FeAsS (Moëlo *et al.* 1987). Owing to the interest in the crystal chemistry of arsenopyrite, it was decided to refine its crystal structure. This refinement has been done in conjunction with a Mössbauer study. The results are presented herein.

Mineralogical Characterization

The quarry at La Roche-Balue is located in the Bouguenais district, southwest of Nantes, Loire-Atlantique department, in France. Leptynitic gneisses of the Pellerin Formation are cut by a quartz vein, up to one meter thick, split in its upper part into centimetric veinlets of quartz and orthoclase (Marcoux 1980). Ore minerals are disseminated within these veinlets. Visible minerals are scheelite, galena and arsenopyrite, with minor pyrite. A detailed reflected-light study also identified sphalerite, chalcopyrite, pyrrhotite, marcasite, molybdenite, native gold and bismuth, and several Pb–Bi and Pb–Ag–Bi sulfosalts (Moëlo *et al.* 1987). A mineral visually identified initially as "grey copper" was later characterized by microprobe as Fe-rich greenockite of primary hydrothermal origin.

Arsenopyrite is generally encountered as millimetric euhedral crystals disseminated in quartz or in the adjacent gneiss (Moëlo *et al.* 1987). Electron-microprobe data were obtained using the synthetic arsenopyrite Asp 200 of Kretschmar & Scott (1976) as a standard.The analyses gave the composition (wt%, mean of 11 spot analyses): Fe 34.02(24), As 47.06(20), S 19.19(19), sum 100.27(42); atom proportions are (%): Fe 33.18(14), As 34.22(18), S 32.60(12). On the basis of As + S = 2 atoms, its structural formula is $Fe_{0.993(4)}As_{1.024(5)}S_{0.976(4)}$, which is close to $FeAs_{1.02}S_{0.98}$.

TABLE 1. ARSENOPYRITE: CRYSTALLOGRAPHIC DATA AND REFINEMENT PARAMETERS

Crystal data	
Ideal formula	FeAsS
Crystal system	monoclinic
Space group	$P2_1/c$
Unit-cell parameters	
a, b, c (Å)	5.7612(8), 5.6841(7), 5.7674(8)
β (°)	111.721(8)
Unit-cell volume (Å^3)	175.46(4)
Z	4
Crystal size (mm)	0.032 × 0.041 × 0.050
Data collection	
Diffractometer	Bruker P4 (point detector)
Temperature (K)	298(3)
Radiation, wavelength (Å)	Mo$K\alpha$, 0.71073
θ range for data collection (°)	1.00 - 35.00
h, k, l ranges	± 9, ± 9, ± 9
scan width (°), scan speed (°/min)	2.70, 1.65
Total reflections collected	3109
Unique reflections (R_{int})	774 (0.0238)
Unique reflections $F > 4\sigma(F)$	758
Absorption correction method	ψ scan (North *et al.* 1968)
Structure refinement	
Refinement method	Full-matrix least-squares on F^2
Twin matrix	$\begin{bmatrix} 0 & 0 & 1 \\ 0 & -1 & 0 \\ 1 & 0 & 0 \end{bmatrix}$
Twin volume fraction	0.476(2)
Data / restraints / parameters	774 / 0 / 29
R_1 [$F_o > 4\sigma(F_o)$]	0.0298
R_1 all	0.0299
Goodness-of-fit on F^2	1.108
Largest diff. peak and hole (e$^-$/Å^3)	1.77, -2.86

$R_{int} = (n / n - 1)^{½} [F_o^2 - F_o\,(mean)^2] / \Sigma F_o^2$
$R_1 = \Sigma \parallel F_o \mid - \mid F_c \parallel / \Sigma \mid F_o \mid$
$GOOF = \{ \Sigma [w (F_o^2 - F_c^2)^2 / (n - p)\}^{½}$, where n is the number of reflections, and p is the number of refined parameters.

Arsenopyrite crystals were extracted from the same hand-size rock sample used for the electron-microprobe study. A part of this sample was broken, and crystal fragments of arsenopyrite were selected under a binocular microscope. Some crystals were crushed for an X-ray powder-diffraction study, which revealed only traces of galena and feldspar (microcline).

TABLE 2. ATOMS, SITE-OCCUPANCY FACTORS, FRACTIONAL COORDINATES (Å), AND EQUIVALENT ISOTROPIC DISPLACEMENT PARAMETERS (Å^2) FOR THE ARSENOPYRITE CRYSTAL SELECTED

atom	occupancy	*x*	*y*	*z*	U_{iso}
Fe	1.00	0.28353(8)	-0.00643(7)	0.29429(9)	0.0155(1)
As	1.00	0.14746(6)	0.13055(5)	0.86937(6)	0.0159(1)
S	1.00	0.6551(2)	0.1311(1)	0.3211(2)	0.0188(2)

Crystal-Structure Study

Experimental and structure refinement

A small fragment of arsenopyrite (0.032 × 0.041 × 0.050 mm in size) was selected from a crushed sample and fixed at the tip of a glass capillary by means of solvent-free glue for the X-ray single-crystal diffraction study. The diffraction quality was checked by means of a Bruker P4 single-crystal diffractometer equipped with a conventional point-detector. Unit-cell dimensions, determined by least-squares refinement of the setting angles of 40 reflections, are: *a* 5.7612(8), *b* 5.6841(7), *c* 5.7674(8) Å, β 111.721(8)°, and *V* 175.46(4) Å^3. To assure merging in all the Laue classes, a full diffraction sphere was collected. Intensities were treated for Lorentz and polarization effects and, subsequently, corrected for absorption following the semi-empirical

TABLE 3. ANISOTROPIC DISPLACEMENT PARAMETERS OF ATOMS IN ARSENOPYRITE

Atom	U_{11}	U_{22}	U_{33}	U_{23}	U_{13}	U_{12}
Fe	0.0155(2)	0.0152(2)	0.0159(2)	0.0003(2)	0.0059(1)	0.0004(1)
As	0.0158(2)	0.0158(2)	0.0162(2)	-0.0002(1)	0.0060(1)	0.0002(1)
S	0.0177(4)	0.0188(3)	0.0201(4)	0.0001(3)	0.0072(3)	-0.0004(3)

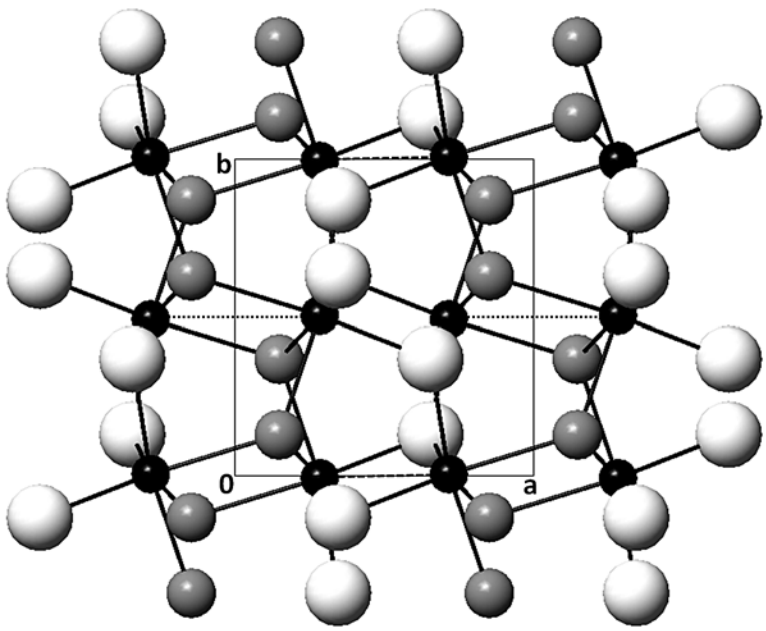

FIG. 1. Projection of the crystal structure of arsenopyrite from La Roche-Balue along the **c** axis. Black, grey and white circles refer to Fe, As and S atoms, respectively. Stippled and dashed lines: long and short Fe–Fe bonds, respectively.

method of North *et al*. (1968). Experimental details of the data collection are given in Table 1.

The structure refinement was performed in space group $P2_1/c$, starting from the atom coordinates of arsenopyrite given by Fuess *et al*. (1987), using the program SHELXL–97 (Sheldrick 2008). The site occupancy for all the sites was left free to vary (atomic species *versus* structural vacancy); all the sites were found to be fully occupied within the analytical uncertainty, without any significant deviation from the stoichiometric formula. Neutral scattering curves for Fe, As, and S were taken from *The International Tables of X-ray Crystallography*, volume IV (Ibers & Hamilton 1974). The refinement was performed following the method of Pratt *et al*. (1971) for twinned structures, assuming twinning on {101}. The introduction of the twinning dramatically lowered the *R* index from 0.2033 to 0.0298 for 758 observed reflections having $F_o > 4\sigma(F_o)$.

Details of the refinement and *R* indices are given in Table 1. Fractional coordinates and isotropic-displacement parameters of atoms are shown in Table 2. Anisotropic displacement parameters and bond distances are given in Tables 3 and 4, respectively. A list of the observed and calculated structure-factors and a cif file are available from the Depository of Unpublished Data, MAC website [document Arsenopyrite CM50_471].

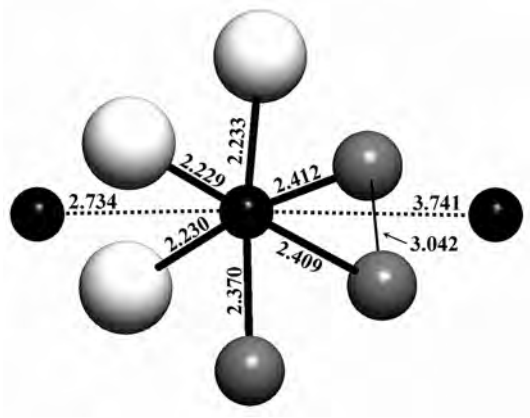

FIG. 2. Coordination of Fe in the crystal structure of arsenopyrite from La Roche-Balue. Symbols as in Figure 1.

Description of the structure

Figure 1 shows the crystal structure of arsenopyrite projected along the **c** axis. All structures of the

TABLE 4. MAIN INTERATOMIC DISTANCES (Å) FOR THE ARSENOPYRITE CRYSTAL SELECTED

Fe	- S	2.229(1)	Fe	- As	2.3702(6)	Fe	- Fe	2.7343(8)
	- S	2.230(1)		- As	2.4093(6)		- Fe	3.7407(4)
	- S	2.2333(9)		- As	2.4123(6)			
As	- S	2.3742(9)	As	- As	3.0422(6)			

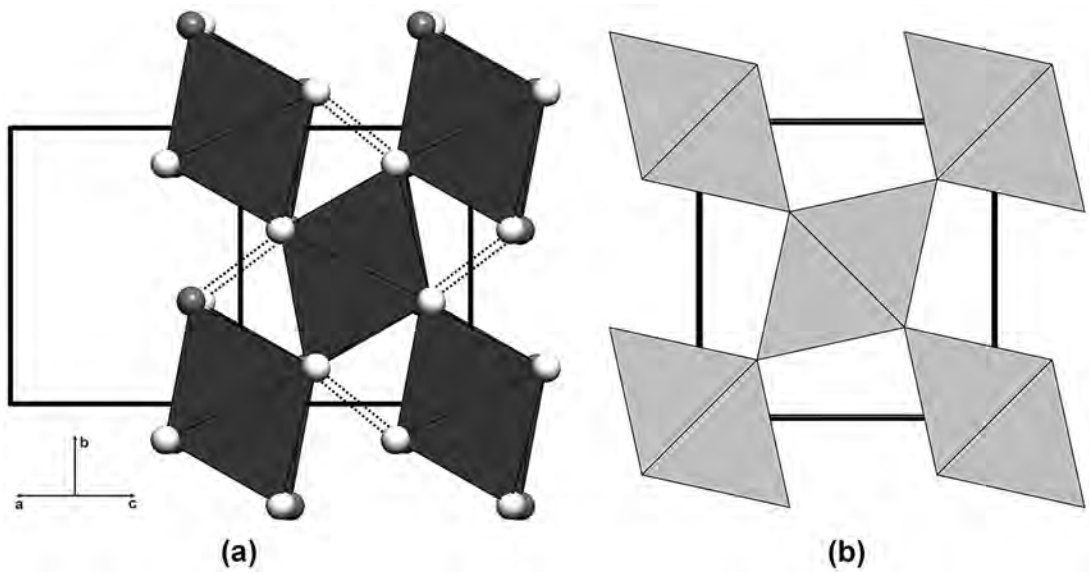

FIG. 3. Projection of the crystal structure of arsenopyrite from La Roche-Balue along [101] (a) compared to that of rutile, TiO_2 (b).

pyrite–marcasite family are characterized by: (*i*) 3D polymerization of MeA_6 octahedra, and (*ii*) all anions form A_2 pairs (Strunz & Nickel 2001). Various symmetries are possible, from cubic to monoclinic. According to Morimoto & Clark (1961), symmetry evolves from orthorhombic to monoclinic for S-rich and As-rich members, respectively. Within this series, the stoichiometric sample that we selected is monoclinic (Table 1).

In the structure, the Fe atoms are octahedrally coordinated by three S and three As atoms (Fig. 2, Table 4); there are also two Fe atoms at 2.734 Å ("short bond") and 3.741 Å ("long bond"), as emphasized by Nickel (1970). The Fe octahedron is asymmetric; in the direction of the Fe–Fe contact, the short Fe–Fe bond cuts the long S–S edge (3.522 Å), whereas the long Fe–Fe bond cuts the short As–As edge (3.042 Å). Correlatively, the S–Fe–S angle is obtuse (104.35°), whereas the As–Fe–As angle is acute (78.24°). The bond length of the As–S pair is 2.374 Å.

The $FeAs_3S_3$ octahedra share two opposite edges to form single strips parallel to [101], with alternation of the short and long Fe–Fe bonds. All the corners connect two strips of octahedra. Figure 3 is the projection of the structure along [101] and shows that the structure of arsenopyrite is a distorted derivative of the archetype rutile, TiO_2 (Wijeyesekera & Hoffmann 1983). The arsenopyrite structure is obtained first by the compression of this archetype with tetragonal symmetry along *a* (or *b*), in order to form the anionic pairs (indicated by stippled lines in Fig. 3). With S alone, it gives the marcasite structure, with orthorhombic symmetry. A second distortion, decreasing the symmetry to monoclinic, visible in Figure 1, is the alternation of slabs of long Fe–Fe bonds and slabs of short Fe–Fe bonds parallel to (100). The close similarity of the arsenopyrite structure with that of the compressed structure of rutile explains the strong orthorhombic pseudosymmetry, as well as the twinning observed in the mineral studied here.

Mössbauer Spectroscopy

Method

The ^{57}Fe Mössbauer spectra were obtained in the constant-acceleration mode and in transmission geometry using a spectrometer composed of devices from Wissel (velocity transducers) and Canberra (interface acquisition) supplier. A room-temperature ^{57}Co(Rh) source has been used. Calibration of the velocity scale was done using absorption lines of iron foil, and isomer shifts are given relative to α-Fe. After folding, the spectra (256 channels) were computed with a least-squares routine using Lorentzian lines.

Taking into account the chemical composition of arsenopyrite, the absorption coefficients of Fe, As and

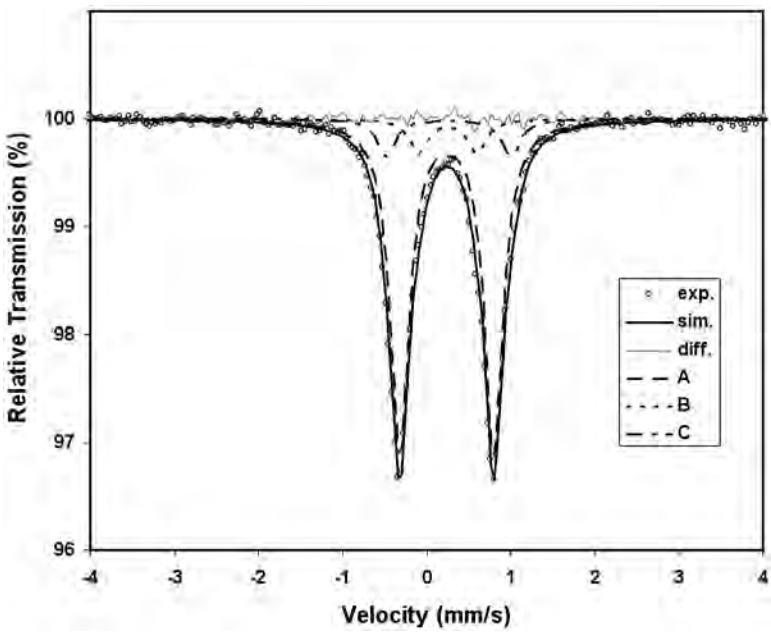

FIG. 4. Mössbauer spectrum for arsenopyrite from La Roche-Balue. A, B and C: three constitutive doublets (dashed, stippled and stippled-dashed lines, respectively); exp.: experimental measurements (circles); sim.: simulated curve (sum of A, B and C; full line); diff.: difference between experimental and simulated curves (grey line).

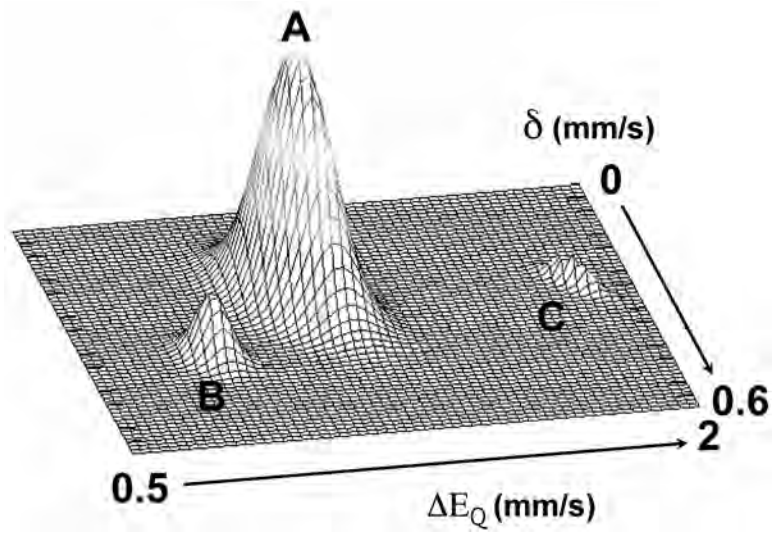

FIG. 5. Two-dimensional site distribution of isomer shift δ *versus* quadrupole splitting ΔE_Q of the Mössbauer spectrum for arsenopyrite from La Roche-Balue.

S, as well as the geometry of the apparatus, the weight of the sample was optimized to 40 mg, corresponding to an effective thickness of 13 mg/cm^2. Arsenopyrite was crushed and mixed with sugar powder in order to be spread homogeneously in the measurement cell. For comparison, three samples of pyrite, marcasite and löllingite were studied according to the same operating conditions (optimal weight: 90 mg for pyrite and marcasite, and 30 mg for löllingite).

Spectra were acquired with a velocity scale of ±4.6 mm/s. The statistical rate for the baseline points of the spectra was 7.7×10^6, with a signal-to-noise ratio of 4×10^{-4}.

Results

The Mössbauer spectrum of arsenopyrite from La Roche-Balue (Fig. 4) shows a doublet with a full-width height (FWH) of 0.32 mm/s, whereas pyrite and marcasite have FWH of 0.27 mm/s. Such a broadening of the Mössbauer spectrum of arsenopyrite was noted first by Imbert *et al.* (1963). For the deconvolution of this spectrum, the dataset was first refined on the basis of a two-dimensional site distribution of isomer shift (step: 0.02 mm/s) and quadrupole splitting (step: 0.05 mm/s). The resulting diagram (Fig. 5) shows three distinct sites ($\chi^2 = 1.7$), in accordance with the results of Murzin *et al.* (2003). This three-site model was used in the final refinement, with the constraint of an identical FWH for the three doublets. The result gives a χ^2 of 0.86, and a FWH of 0.27 mm/s.

Parameters of the doublets of the Mössbauer spectra of arsenopyrite from La Roche-Balue, pyrite, marcasite and löllingite are given in Table 5. Values of the isomer shift (δ) and quadrupole splitting (ΔE_Q) of pyrite and marcasite are close to those obtained initially by Imbert *et al.* (1963) and Evans *et al.* (1982, and references therein). Table 5 also compares δ, ΔE_Q, and relative area *S* of the three doublets A, B and C of arsenopyrite from La Roche-Balue with the values obtained by Murzin *et al.* (2003) for samples BB–14 and OK–2, whose compositions are close to being stoichiometric [S/As (at.) = 0.98 and 1.01, respectively]. There is a general concordance of the new data with those of Murzin *et al.* (2003), not only regarding δ and ΔE_Q values, but also the relative *S* values of the three constitutive doublets. Our data also confirm that relative to the main doublet A, ΔE_Q of the minor doublet B is shifted toward ΔE_Q of the marcasite doublet, whereas concomitantly ΔE_Q of the second minor doublet C is shifted toward ΔE_Q of the löllingite doublet (Table 5). All three doublets correspond to divalent Fe at the low-spin state in an octahedral environment, as demonstrated by Nickel (1968).

DISCUSSION

Although the microprobe analysis gave a slight excess of As over S, the crystal-structure study presented here points to a stoichiometric composition, without significant deviation of the As:S ratio from unity. This finding may signify that the standard Asp200 used for the microprobe analysis had a nominal As:S ratio given by Kretschmar & Scott (1976) slightly

higher than the true one, inducing a slight overestimation of the measured As:S ratio of arsenopyrite from La Roche-Balue.

Fuess *et al*. (1987) have compared previous crystal-structure data of arsenopyrite (not including, however, those of Bonnemère & Wintenberger 1961). In Table 6, such a comparison is focused on interatomic distances, volumes and *R* factors. It shows the heterogeneity of datasets; they do not permit us to draw any conclusion from the variations of interatomic distances or unit-cell volumes. The only precise resolution before this study is that of Fuess *et al*. (1987), with a low *R*-factor and with indication of the As:S ratio below that of arsenopyrite from La Roche-Balue. This explains its lower volume (349.5 *versus* 350.9 Å^3), but the effect of a significant content of Co substituting for Fe (0.12 *apfu* Co) on the variation of the volume as well as interatomic distances cannot be neglected.

TABLE 5. MÖSSBAUER PARAMETERS OF SAMPLES STUDIED (ARSENOPYRITE FROM LA ROCHE-BALUE; PYRITE; MARCASITE) COMPARED TO PREVIOUS DATA

Deposit	S:As		δ (mm/s)	ΔE_Q (mm/s)	*S* (%)	Source
Pyrite						
Mexico			0.31(1)	0.60(2)		This study
Mean value			0.313(8)	0.611(3)		Evans *et al.* (1982)
Marcasite						
France			0.27(1)	0.50(2)		This study
Mean value			0.277(2)	0.503(7)		Evans *et al.* (1982)
Arsenopyrite						
Provenance unknown			0.34	1.05		Imbert *et al.* (1963)
La Roche-Balue	1.00	A	0.24(1)	1.12(2)	82(3)	This study
		B	0.25(1)	0.69(2)	8.5(1.0)	
		C	0.26(1)	1.49(2)	9.3(1.0)	
Kotchkarskoe	0.98	A	0.238(1)	1.115(1)	89.3	Murzin *et al.* (2003)
BB-14		B	0.253(3)	0.695(8)	6.6	
		C	0.223(5)	1.55(1)	4.1	
Kotchkarskoe	1.01	A	0.241(1)	1.115(2)	81.8	Murzin *et al.* (2003)
OK-2		B	0.296(2)	0.617(5)	13.0	
		C	0.248(6)	1.52(3)	5.2	
Löllingite						
Provenance unknown			0.30	1.68		Imbert *et al.* (1963)
Brazil			0.29(1)	1.73(2)		This study

A, B, C: three doublets within the same sample. *S* (%): relative area.

TABLE 6. COMPARISON OF INTERATOMIC DISTANCES (Å), VOLUMES (Å^3, Z = 8) AND *R* FACTORS FOR ARSENOPYRITE CRYSTALS

Ref.	Symmetry	As:S	Fe–S*	Fe–As*	As–S	Fe–Fe**	Fe–Fe***	*V*	R_{struct}
(1)	monoclinic	?	2.263	2.356	2.304	2.894	3.537	346.8	no R
(2)	monoclinic		2.204	2.402	2.417	2.639	3.795	346.8	0.3
(2)	triclinic	0.96:1.04	2.246(4)	2.371(4)	2.326(4)	2.819(4)	3.618(4)	349.3(3)	0.245
			2.265	2.364	2.338	2.827	3.614		
(3)	triclinic	?	2.197	2.368	2.242	2.635	3.790	345.0	0.3
			2.275	2.382	2.412	2.943	3.482		
(4)	monoclinic	0.88:1.12	2.254(1)	2.363(1)	2.345(1)	2.922(1)	3.627(1)	349.5(1)	0.04
(5)	monoclinic	1.00:1.00	2.2306(10)	2.3973(6)	2.3742(9)	2.7343(8)	3.7407(4)	350.92(8)	0.0299

(1) Buerger (1936), (2) Morimoto & Clark (1961), (3) Bonnemère & Wintenberger (1961), (4) Fuess *et al.* (1987), (5) This study. Triclinic: Two Fe, As and S positions. * mean of three bonds; ** shortest Fe–Fe distance; *** second Fe–Fe distance.

The most interesting aspect of the study is the apparent contradiction between the results of the crystal-structure study and those of Mössbauer spectroscopy, even if one takes into account the accuracies of the two methods. Although the crystal-structure analysis indicates unmixed Fe, As and S sites, corresponding to an average octahedral environment of the Fe atoms, the Mössbauer spectrum indicates three distinct Fe environments. Imbert *et al.* (1963) first pointed out the broadening of the two peaks of the arsenopyrite spectrum relative to those of pyrite and löllingite, which broadening was interpreted as the sum of two close doublets. Murzin *et al.* (2003) proved the coexistence of three doublets, independently of the As:S ratio (with an additional singlet for S-rich samples). These authors concluded that such a feature is likely due to the coexistence of three non-equivalent positions of Fe atoms in the arsenopyrite structure, and proposed that each of them can be shown as a combination of polyhedra with definite sets of S and As atoms "dissolved" in the structure without forming their own mineral phases.

According to Table 5, our results are in very good agreement with the data of Murzin *et al.* (2003), and confirm the presence of Fe non-equivalent positions, formed in a similar manner in a quite distinct ore deposit. The crystal-structure study of stoichiometric arsenopyrite from La Roche-Balue shows that mutual (and symmetric) As ↔ S substitutions at the As and S positions, which would have changed the As:S ratio for a significant percentage among the Fe octahedra, did not occur.

The exact origin of the complexity of Fe environment remains uncertain. Two likely alternatives are: 1) local disorder of Fe coordination beyond well-crystallized arsenopyrite domains (crystal surfaces and joints; twin walls), or 2) very weak departure of the crystal structure from the monoclinic symmetry not revealed by the X-ray-diffraction study. The first alternative seems the more attractive. According to crystallographic studies (Buerger 1936, Fuess *et al.* 1987) as well as routine metallographic observations (with crossed polars), a very fine twinning is ubiquitous in arsenopyrite. As illustrated by Figure 5 of Fuess *et al.* (1987), twinning at the atom scale induces antiphase-domain boundaries where the coordination of Fe is changed: $FeAs_2S_4$ and reverse $FeAs_4S_2$ octahedra, as well as $FeAsS_5$ and reverse $FeAs_5S$ octahedra. The two minor doublets B and C of the Mössbauer spectrum of arsenopyrite from La Roche-Balue may correspond to one of these two pairs of octahedra, in accordance with the shifts of ΔE_{QB} and ΔE_{QC} toward ΔE_Q of marcasite and löllingite, respectively. Such a significant shift in two opposite directions is more difficult to explain by a symmetry decrease from a monoclinic to a triclinic distortion.

According to this hypothesis, whereas the main A doublet would correspond to the "normal" $FeAs_3S_3$ octahedron, the quite equal ratios of S_B and S_C, which would be related to a definite pair of octahedra, will not change significantly the As:S ratio. Nevertheless, as the sum of S_B and S_C reaches about 20% of the Fe octahedra of the whole structure, it is peculiar that it had no incidence on the observed X-ray single-crystal data.

Conclusions

Together with the study of Fuess *et al.* (1987), the study of arsenopyrite from La Roche-Balue is the second accurate crystal-structure refinement of this mineral (combination of a good *R*-factor together with a precise As:S ratio). Moreover, it corresponds to a quite pure, stoichiometric FeAsS. It thus constitutes a good basis for the acquisition or calculation of thermochemical data on this mineral, whose oxidation in natural conditions or in mine wastes is the main factor of aqueous contamination by soluble arsenic.

As revealed initially by Murzin *et al.* (2003), the ^{57}Fe Mössbauer spectroscopic study presented here, on a new sample of arsenopyrite, confirms the three non-equivalent positions of Fe atoms, on the basis of quite distinct values of the quadrupole splitting ΔE_Q. Such a crystal-chemical complexity appears as an intrinsic characteristic of arsenopyrite, which likely results from the distribution of Fe atoms among distinct $FeAs_nS_m$ octahedra, rather than to different distortions of the basic $FeAs_3S_3$ octahedron.

To validate this hypothesis, it will be necessary to continue such a Mössbauer study, correlated to crystal-chemical characterization (especially for samples with the greatest departure from stoichiometry). Such a study is under way. Also, HRTEM studies appear necessary to correlate the As:S ratio with parameters such as twin laws, size of twin domains controlling the density of twin defects (*i.e.*, distribution of different Fe coordinations), and possible triclinic symmetry. This approach may be also a prerequisite to understand the distribution of gold at the atom scale in Au-rich arsenopyrite: are the gold atoms diluted in ordered crystal domains (*i.e.*, with normal $FeAs_3S_3$ octahedra) or fixed by defects with a specific dissymmetric coordination of Fe?

Acknowledgements

We sincerely thank V.V. Murzin (Institute of Geology and Geochemistry, Ekaterinburg) and P.G. Spry (Iowa State University) for their constructive comments. The help of T. Balić-Žunić, guest editor, and R.F. Martin is very much appreciated.

LB is really glad to contribute to this issue dedicated to Emil Makovicky, one of the most prominent figures in mineralogical crystallography. LB had the pleasure of collaborating with him in recent years on the structural characterization of complex new minerals. As usual, Emil gave a very remarkable contribution. His long-standing studies on the crystal chemistry of sulfides and sulfosalts (and related minerals) are especially

noteworthy, and they undoubtedly represent a solid basis for the next generations. Emil perfectly symbolizes the ideal bridge between mineralogy and the most advanced fields of crystallography.

References

Bonnemère, C. & Winterberger, M. (1961): Sur la structure cristalline de l'arsénopyrite. *C.R. Acad. Sci. Paris* **252**, 1344-1346.

Buerger, M.J. (1936): The symmetry and crystal structure of the minerals of the arsenopyrite group. *Z. Kristallogr.* **95**, 83-113.

Cipriani, C., Borrini, D. & Mazzetti, G. (1998): Revisione della collezione di arsenopiriti del Museo di Mineralogia dell'Università di Firenze. *Mus. Scient.* **14**, 219-228.

Evans, B.J., Johnson, R.G., Senftle, F.E., Blaine Cecil, C. & Dulong, F. (1982): The ^{57}Fe Mössbauer parameters of pyrite and marcasite with different provenances. *Geochim. Cosmochim. Acta* **46**, 761-775.

Fuess, H., Kratz, T., Topel-Schadt, J. & Miehe, G. (1987): Crystal structure refinement and electron microscopy of arsenopyrite. *Z. Kristallogr.* **179**, 335-346.

Ibers, J.A. & Hamilton, W.C., eds. (1974): *International Tables for X-Ray Crystallography*, vol. IV. Kynoch Press, Dordrecht, The Netherlands.

Imbert, P., Gérard, A. & Winterberger, M. (1963): Etude des sulfure, arséniosulfure et arséniure de fer naturels par effet Mössbauer. *C.R. Acad. Sci. Paris* **256**, 4391-4394.

Kretschmar, U. & Scott, S.D. (1976): Phase relations involving arsenopyrite in the system Fe–As–S and their application. *Can. Mineral.* **14**, 364-386.

Marcoux, E. (1980): *Le district de Pontivy. Sa place dans la métallogénie plombo-zincifère du Massif Armoricain (France)*. Thesis no. 636, Université de Clermont II, Clermont-Ferrand, France.

Moëlo, Y., Marcoux, E., Makovicky, E., Karup-Møller, S. & Legendre, O. (1987): Homologues de la lillianite (gustavite, vikingite, heyrovskyite riche en Ag et Bi...) de l'indice à W–As–(Pb,Bi,Ag) de La Roche-Balue (Loire-Atlantique, France). *Bull. Minéral.* **110**, 43-64.

Morimoto, N. & Clark, L.A. (1961): Arsenopyrite crystal-chemical relations. *Am. Mineral.* **46**, 1448-1469.

Murzin, V.V., Semenkin, V.A., Sustavov, S.G, Krinov, D.I., Pikulev, A.I. & Milder, O.B. (2003): Non-equivalent positions of Fe atoms in gold bearing arsenopyrite according to Mössbauer spectroscopy. *Geokhimiya* **8**, 1-9 (in Russian).

Nickel, E.H. (1968): Structural stability of minerals with the pyrite, marcasite, arsenopyrite and löllingite structures. *Can. Mineral.* **9**, 311-321.

Nickel, E.H. (1970): The application of ligand-field concepts to an understanding of the structural stabilities and solid-solution limits of sulphides and related minerals. *Chem. Geol.* **5**, 233-241.

North, A.C.T., Phillips, D.C. & Mathews, F.S. (1968): A semi-empirical method of absorption correction. *Acta Crystallogr.* **A24**, 351-359.

Pratt, C.S., Coyle, B.A. & Ibers, J.A. (1971): Redetermination of the structure nitrosylpenta-amminecobalt (III) dichloride. *J. Chem. Soc.* (*A*), 2146-2151.

Sheldrick, G.M. (2008): A short history of SHELX. *Acta Crystallogr.* **A64**, 112-122.

Strunz, H. & Nickel, E.H. (2001): *Strunz Mineralogical Tables* (9th ed.). Schweizerbart, Stuttgart, Germany.

Wijeyesekera, S.D. & Hoffmann, R. (1983): Marcasites and arsenopyrites: structure, bonding and electrical properties. *Inorg. Chem.* **22**, 3287-3300.

Received April 7, 2011, revised manuscript accepted March 18, 2012.

```
data_rb-orl_arsenopyrite

_audit_creation_method            SHELXL-97
_chemical_name_systematic
;
 ?
;
_chemical_name_common             ?
_chemical_melting_point           ?
_chemical_formula_moiety          ?
_chemical_formula_sum
 'As Fe S'
_chemical_formula_weight          162.83

loop_
 _atom_type_symbol
 _atom_type_description
 _atom_type_scat_dispersion_real
 _atom_type_scat_dispersion_imag
 _atom_type_scat_source
 'As'  'As'   0.0499   2.0058
 'International Tables Vol C Tables 4.2.6.8 and 6.1.1.4'
 'Fe'  'Fe'   0.3463   0.8444
 'International Tables Vol C Tables 4.2.6.8 and 6.1.1.4'
 'S'  'S'   0.1246   0.1234
 'International Tables Vol C Tables 4.2.6.8 and 6.1.1.4'

_symmetry_cell_setting            ?
_symmetry_space_group_name_H-M    ?

loop_
 _symmetry_equiv_pos_as_xyz
 'x, y, z'
 '-x, y+1/2, -z+1/2'
 '-x, -y, -z'
 'x, -y-1/2, z-1/2'

_cell_length_a                    5.7612(8)
_cell_length_b                    5.6841(7)
_cell_length_c                    5.7674(8)
_cell_angle_alpha                 90.00
_cell_angle_beta                  111.721(8)
_cell_angle_gamma                 90.00
_cell_volume                      175.46(4)
_cell_formula_units_Z             4
_cell_measurement_temperature     298(2)
_cell_measurement_reflns_used     ?
_cell_measurement_theta_min       ?
_cell_measurement_theta_max       ?

_exptl_crystal_description        ?
_exptl_crystal_colour             ?
_exptl_crystal_size_max           ?
_exptl_crystal_size_mid           ?
```

```
_exptl_crystal_size_min           ?
_exptl_crystal_density_meas       ?
_exptl_crystal_density_diffrn     6.164
_exptl_crystal_density_method     'not measured'
_exptl_crystal_F_000              300
_exptl_absorpt_coefficient_mu     27.909
_exptl_absorpt_correction_type    ?
_exptl_absorpt_correction_T_min   ?
_exptl_absorpt_correction_T_max   ?
_exptl_absorpt_process_details    ?

_exptl_special_details
;
 ?
;

_diffrn_ambient_temperature       293(2)
_diffrn_radiation_wavelength      0.71073
_diffrn_radiation_type            MoK\a
_diffrn_radiation_source          'fine-focus sealed tube'
_diffrn_radiation_monochromator   graphite
_diffrn_measurement_device_type   ?
_diffrn_measurement_method        ?
_diffrn_detector_area_resol_mean  ?
_diffrn_standards_number          ?
_diffrn_standards_interval_count  ?
_diffrn_standards_interval_time   ?
_diffrn_standards_decay_%         ?
_diffrn_reflns_number             3109
_diffrn_reflns_av_R_equivalents   0.0238
_diffrn_reflns_av_sigmaI/netI     0.0630
_diffrn_reflns_limit_h_min        -9
_diffrn_reflns_limit_h_max        9
_diffrn_reflns_limit_k_min        -9
_diffrn_reflns_limit_k_max        9
_diffrn_reflns_limit_l_min        -9
_diffrn_reflns_limit_l_max        9
_diffrn_reflns_theta_min          1.81
_diffrn_reflns_theta_max          34.98
_reflns_number_total              774
_reflns_number_gt                 758
_reflns_threshold_expression      >2sigma(I)

_computing_data_collection        ?
_computing_cell_refinement        ?
_computing_data_reduction         ?
_computing_structure_solution     ?
_computing_structure_refinement   'SHELXL-97 (Sheldrick, 1997)'
_computing_molecular_graphics     ?
_computing_publication_material   ?

_refine_special_details
;
 Refinement of F^2^ against ALL reflections.  The weighted R-factor wR and
 goodness of fit S are based on F^2^, conventional R-factors R are based
```

```
 on F, with F set to zero for negative F^2^. The threshold expression of
 F^2^ > 2sigma(F^2^) is used only for calculating R-factors(gt) etc. and is
 not relevant to the choice of reflections for refinement.  R-factors based
 on F^2^ are statistically about twice as large as those based on F, and R-
 factors based on ALL data will be even larger.
;

_refine_ls_structure_factor_coef  Fsqd
_refine_ls_matrix_type            full
_refine_ls_weighting_scheme       calc
_refine_ls_weighting_details
 'calc w=1/[\s^2^(Fo^2^)+(0.0230P)^2^+0.0000P] where P=(Fo^2^+2Fc^2^)/3'
_atom_sites_solution_primary      direct
_atom_sites_solution_secondary    difmap
_atom_sites_solution_hydrogens    geom
_refine_ls_hydrogen_treatment     mixed
_refine_ls_extinction_method      none
_refine_ls_extinction_coef        ?
_refine_ls_number_reflns          774
_refine_ls_number_parameters      29
_refine_ls_number_restraints      0
_refine_ls_R_factor_all           0.0299
_refine_ls_R_factor_gt            0.0298
_refine_ls_wR_factor_ref          0.0717
_refine_ls_wR_factor_gt           0.0717
_refine_ls_goodness_of_fit_ref    1.108
_refine_ls_restrained_S_all       1.108
_refine_ls_shift/su_max           0.000
_refine_ls_shift/su_mean          0.000

loop_
 _atom_site_label
 _atom_site_type_symbol
 _atom_site_fract_x
 _atom_site_fract_y
 _atom_site_fract_z
 _atom_site_U_iso_or_equiv
 _atom_site_adp_type
 _atom_site_occupancy
 _atom_site_symmetry_multiplicity
 _atom_site_calc_flag
 _atom_site_refinement_flags
 _atom_site_disorder_assembly
 _atom_site_disorder_group
Fe Fe 0.28353(8) -0.00643(7) 0.29429(9) 0.01553(11) Uani 1 1 d . . .
As As 0.14746(6) 0.13055(5) 0.86937(6) 0.01590(11) Uani 1 1 d . . .
S S 0.65506(15) 0.13106(12) 0.32107(17) 0.01879(16) Uani 1 1 d . . .

loop_
 _atom_site_aniso_label
 _atom_site_aniso_U_11
 _atom_site_aniso_U_22
 _atom_site_aniso_U_33
 _atom_site_aniso_U_23
 _atom_site_aniso_U_13
```

```
 _atom_site_aniso_U_12
Fe 0.0155(2) 0.01519(18) 0.0159(2) 0.00027(15) 0.00594(13) 0.00043(14)
As 0.01578(19) 0.01576(15) 0.0162(2) -0.00015(10) 0.00596(11) 0.00015(10)
S 0.0177(4) 0.0188(3) 0.0201(4) 0.0001(3) 0.0072(2) -0.0004(2)

_geom_special_details
;
 All esds (except the esd in the dihedral angle between two l.s. planes)
 are estimated using the full covariance matrix.  The cell esds are taken
 into account individually in the estimation of esds in distances, angles
 and torsion angles; correlations between esds in cell parameters are only
 used when they are defined by crystal symmetry.  An approximate (isotropic)
 treatment of cell esds is used for estimating esds involving l.s. planes.
;

loop_
 _geom_bond_atom_site_label_1
 _geom_bond_atom_site_label_2
 _geom_bond_distance
 _geom_bond_site_symmetry_2
 _geom_bond_publ_flag
Fe S 2.2287(10) 3_656 ?
Fe S 2.2297(10) . ?
Fe S 2.2333(9) 2_645 ?
Fe As 2.3702(6) 4_565 ?
Fe As 2.4093(6) 1_554 ?
Fe As 2.4123(6) 3_556 ?
Fe Fe 2.7343(8) 3_656 ?
As Fe 2.3702(6) 4_566 ?
As S 2.3742(9) 3_656 ?
As Fe 2.4093(6) 1_556 ?
As Fe 2.4123(6) 3_556 ?
S Fe 2.2287(10) 3_656 ?
S Fe 2.2333(9) 2_655 ?
S As 2.3742(9) 3_656 ?

loop_
 _geom_angle_atom_site_label_1
 _geom_angle_atom_site_label_2
 _geom_angle_atom_site_label_3
 _geom_angle
 _geom_angle_site_symmetry_1
 _geom_angle_site_symmetry_3
 _geom_angle_publ_flag
S Fe S 104.35(3) 3_656 . ?
S Fe S 91.09(2) 3_656 2_645 ?
S Fe S 95.17(3) . 2_645 ?
S Fe As 92.64(3) 3_656 4_565 ?
S Fe As 92.60(3) . 4_565 ?
S Fe As 170.28(3) 2_645 4_565 ?
S Fe As 170.83(3) 3_656 1_554 ?
S Fe As 84.25(3) . 1_554 ?
S Fe As 91.31(3) 2_645 1_554 ?
As Fe As 83.650(15) 4_565 1_554 ?
S Fe As 93.31(3) 3_656 3_556 ?
```

```
S Fe As 162.24(4) . 3_556 ?
S Fe As 82.37(3) 2_645 3_556 ?
As Fe As 88.452(18) 4_565 3_556 ?
As Fe As 78.24(2) 1_554 3_556 ?
S Fe Fe 52.19(3) 3_656 3_656 ?
S Fe Fe 52.16(3) . 3_656 ?
S Fe Fe 95.11(3) 2_645 3_656 ?
As Fe Fe 94.27(2) 4_565 3_656 ?
As Fe Fe 136.30(3) 1_554 3_656 ?
As Fe Fe 145.45(4) 3_556 3_656 ?
Fe As S 103.45(3) 4_566 3_656 ?
Fe As Fe 118.165(19) 4_566 1_556 ?
S As Fe 103.70(2) 3_656 1_556 ?
Fe As Fe 123.660(18) 4_566 3_556 ?
S As Fe 103.64(2) 3_656 3_556 ?
Fe As Fe 101.76(2) 1_556 3_556 ?
Fe S Fe 75.65(3) 3_656 . ?
Fe S Fe 127.27(4) 3_656 2_655 ?
Fe S Fe 123.82(4) . 2_655 ?
Fe S As 109.55(3) 3_656 3_656 ?
Fe S As 111.13(3) . 3_656 ?
Fe S As 106.51(4) 2_655 3_656 ?

_diffrn_measured_fraction_theta_max    1.000
_diffrn_reflns_theta_full              34.98
_diffrn_measured_fraction_theta_full   1.000
_refine_diff_density_max    1.773
_refine_diff_density_min   -2.862
_refine_diff_density_rms    0.342
```